

this paper which show columns under E field and static conditions but under shear do not show lamellar particulate structures and none show significant, if any, ER activity. However we feel we have performed sufficient studies , as illustrated here for two situations, to make the following statement with a high degree of confidence. It is a distinguishing characteristic of ER active suspensions that under the combined effect of electric and shear fields , not parallel to each other, that the particles aggregate or regiments into lamellar structures, the long dimension being in the shear direction. The height of the lamellae are arbitrarily chosen to be the distance between the electrodes and in the field direction.

Although the phenomenon presented here is unquestionable there is little known about it other than the mechanisms for interaction between the particles, i.e. induced dipoles in the particles and/or the current through the suspension, and even these are not totally resolved. Questions such as what determines the diameter of the columns, the width of the lamellae, the general periodic spacing of the lamellae and how they evolve with time of shearing are generally unknown and many are under current study. Further, how if at all these lamellar structures are important in the ER phenomenon is still to be determined although it has been hypothesized⁴ that these lamellar structures slip at the electrode surface under shear as opposed to breaking between the electrodes. The types and characteristics of the particles and the matrix fluid, the concentration, the character of the electrodes and gap, the shear rate and time of shearing, the magnitude and character (AC, DC) of the electric field are all parameters which are apparently related in still to be determined ways to the column breadth and the character of the lamellae. Thus the reasons the diameter of the columns and the types of rings are different in the figures cannot at this time be explained, nor can generally be reproduced.

References

1. G. Bossis, Y. Grasselli, E. Lemaire, J. Persillo, L. Petit, "Phase separation and flow induced anisotropy in electro rheological fluids", *Europhysics Lett.* 25(5), 335-340(1994).
2. S. Cuitillas, and G.Bossis,"A comparison between flow-induced structures in electro rheological and magnetorheological fluids" *Europhys.Letters* 40 (4),PP 465-470(1997).
3. S. Cuitillas, G.Bossis, A.Cobers, E.L.Kemaire, A.Meunier, "Field and flow induced structures in relation to the rheology of ER and MR fluids", in *ER Fluids, MR Suspensions, and their Applications*, ed. M. Nakano and K.Koyama, World Scientific, Singapore(1998).
4. S. Henley, and F.E. Filisko, "Flow profiles of ER suspensions: An alternative model for ER activity" *J.Rheol.* 43(5), 1323-1336(1999).
5. X. Tang, W.H.Li, X.J.Wang, P.Q.Zhang,"Structure evolution of ER fluids under flow conditions", in *ER Fluids, MR Suspensions, and their Applications*, ed. M.Nakano and K.Koyama, 164-171, World Scientific, Singapore(1998).
6. M. Whittle,"Computer simulation of an ER fluid" *J. Non Newt. Fluid Mechanics* 37, 233-263(1990).
7. J.R. Melrose,"Brownian dynamics simulation of dipole suspensions under shear: the phase diagram", *Molecular Phys.* 76(3), 635-660(1992).
8. J.R. Melrose, and D.M.Heyes," Simulation of ER and particle mixture suspensions: agglomeration and layered structures", *J. Chem. Phys.* 98(7), 5873-5886(1993).
9. J. Takimoto Computer Simulation of Model Electro rheological Fluids, *Electro rheological Fluids - Mechanisms, Properties, Structure, Technology, and Applications*, 53-58 (1991)
10. U. Treasurer, Radzilowski,L.H. and F.E.Filisko," Polyelectrolytes as inclusions in electro rheologically active materials: Effect of chemical characteristics on ER activity", *J.Rheol.* 35(6), 1051(1991).

CHAIN ROTATIONAL DYNAMICS IN MR SUSPENSIONS

SONIA MELLE^{1,2}, OSCAR G. CALDERÓN³, MIGUEL A. RUBIO¹,

AND GERALD G. FULLER²

¹Dpto. Física Fundamental, UNED, Senda del Rey 9, Madrid 28040, Spain
E-mail: smelle@fisfun.uned.es; mar@fisfun.uned.es

²Dpt. Chemical Engineering, Stanford University, Stanford, CA 94305-5025, USA
E-mail: smelle@chemeng.stanford.edu; ggf@chemeng.stanford.edu

³Dpto. Óptica, UCM, Ciudad Universitaria s/n, Madrid 28040, Spain
E-mail: oscargc@eucmax.sim.ucm.es

The dynamics of induced dipolar chains in magnetorheological suspensions subject to rotating magnetic fields has been experimentally studied combining scattering dichroism and video microscopy experiments. When a rotating field is imposed the chainlike aggregates rotate synchronously with the magnetic field. We found that the average size of the aggregates decreases with Mason number (ratio of viscous to magnetic forces) following a power law with exponent -0.5 being the hydrodynamic friction forces the cause of the chains break up. However the total number of aggregated particles shows two different behaviors depending on Mason number. For low Mason numbers, the total number of aggregated particles remains almost constant and above a critical Mason number, the rotation of the field prevents the particle aggregation process from taking place so the number of aggregated particles decreases with Mason number following a power law behavior with exponent -1. Athermal molecular dynamics simulations are also reported, showing good agreement with the experiments.

Introduction

Magnetic fluids exhibit interesting dynamical behavior when subjected to rotating magnetic fields as has been reported in previous experimental studies on magnetic holes [1,2] and magnetic droplets [3,4]. These systems show synchronous and non-synchronous regimes depending on the value of the driving frequency. J.C. Bacri et al. [3] found unexpected spiny, starfish shaped magnetic microdroplets when a high frequency rotating magnetic field was applied. At lower frequencies, O. Sandre et al. [4] found that the magnetic droplets break up to decrease their viscous drag and facilitate tracking the field rotation. Computer simulations of colloidal suspensions subjected to high frequency biaxial fields have been developed by J.E. Martin et al. [5-7]. They predicted the formation of 2D sheetlike structures aligned in the field plane.

In a previous work [8,9], we used scattering dichroism to study the orientation dynamics of low concentration magnetorheological (MR) suspensions ($\phi \sim 0.01$) when rotating magnetic fields of moderate frequencies (up to 10 Hz) were applied. In these suspensions, dichroism arises from the formation of optically anisotropic chains upon imposition of the magnetic field and gives information about the number of aggregated particles, N. In these experiments we simultaneously measured the dichroism (Δn) and the orientation angle of the structures. We found that the induced chain-like aggregates rotate synchronously with the field but lag behind with a constant phase angle α . Furthermore, two different behaviors were found below or above a critical frequency.

Below this value, the dichroism remains almost constant but above the critical frequency, the viscous drag overcomes the magnetic force and reduces the dichroism following a power law with an exponent approximately -1.

In this work, scattering dichroism and video microscopy experiments have been combined to study the dynamics of induced dipolar chains in MR suspensions subject to rotating magnetic fields. Using scattering dichroism we studied the interplay between magnetic and viscous forces over the critical frequency separating these two regions. A dimensionless parameter that compares these two forces is the well-known Mason number (ratio of viscous to magnetic forces). This number has been defined with different proportionality factors in literature [10-12]. We have adopted the following definition:

$$Ma = \frac{12^2 \eta \omega}{\mu_0 M^2}, \quad (1)$$

where η is the solvent viscosity, ω is the field rotation frequency, M is the particle magnetization, and μ_0 is the vacuum magnetic permeability. We obtained a linear dependence of the critical frequency with the square of the magnetization and the inverse of the viscosity indicating that the Mason number governs the rotational dynamics. Consequently, we find a critical Mason number below which the dichroism remains almost constant and above which the viscous drag prevents the particle aggregation process from taking place.

We have also performed video microscopy experiments to visualize the dynamics of chains for a range of Mason numbers around the critical value (where both magnetic interaction and viscous drag are comparable). Direct observations show that chains rotate synchronously with the field adjusting their size to decrease the viscous drag. We find that the average size of the structures decreases with Ma following a power law with exponent close to -0.5 being the hydrodynamic forces the cause of the chains break up. However the total number of aggregated particles shows two different behaviors depending on Mason number in agreement with scattering dichroism experiments. Our experimental findings have been interpreted also with the help of athermal molecular dynamics simulations that show good agreement with the experimental results.

2 Materials and procedure

The experiments were performed using three suspensions of super-paramagnetic particles obtained diluting 10 % in weight suspensions supplied by *Estapor* (ref. MI-180/12, MI-070/60a and MI-070/60b). The particles contain magnetite crystals Fe_3O_4 of small diameter (1-20 nm) dispersed in a monomer and polymerized using an emulsion process. The surface of the latex micro-spheres is composed of carboxylic acid (-COOH) groups with a surfactant coating layer of sodium dodecyl sulfate (SDS) to stabilize the dispersions. Due to their small average diameter and density ($\rho_p \sim 1.3$ g/ml) the sedimentation time (sedimentation velocity $v_s \sim 0.02$ $\mu m/s$) is long enough to neglect gravitational effects. The properties of the suspensions used in the experiments are detailed in Table 1.

Because the techniques we are using need optical transparency, the suspension was sandwiched between two circular quartz windows with diameter 6.5 mm, separated 100 μm along the vertical optical axis and held in place by a delrin attachment. The sample is surrounded by two orthogonal pairs of coils that generate rotating magnetic fields in the plane orthogonal to the optical axis. All experiments were performed at a temperature $T = 282 \pm 1$ K.

Table 1. Properties of the magnetic suspension used in the experiments.

Experiment	Dichroism	Dichroism	Microscopy
Suspension name	d-MI-180/12	d-MI-70/60a	d-MI-70/60b
Particle mean diameter	1.01 μm	0.90 μm	1.24 μm
Particle magnetic content	13.0 %	62.0 %	61.0 %
Particle polymer nature	PS	PS	PS
Particle surface group content	20 $\mu eq/g$	145 $\mu eq/g$	117 $\mu eq/g$
Particle saturation magnetization	12 emu/g	52.7 emu/g	52 emu/g
Suspension volume fraction	0.016	0.01	0.0001
Suspension glycerol content	82.5 %	40-80 %	0 %

A full description of the scattering dichroism technique can be found in Refs. [8,13]. To perform video microscopy experiments we illuminated the sample from the top using a light source with flexible bundle. To amplify the images, we used a zoom system *Navitar* 12X with which a resolution of 0.34-4.2 μm for field of view around 170-2100 μm can be achieved. The images were recorded with a CCD video camera *Sanyo* VDC-3825 connected to a S-VHS VCR *Panasonic* AG 1975. We digitalized single frames on a computer for their subsequent analysis.

3 Experimental results

3.1 Scattering Dichroism Results

As we showed previously [8], two different behaviors for the dichroism and the phase lag are found below or above a critical frequency. We have studied the dependence of the critical frequency on the magnetization by applying magnetic fields with different amplitudes on suspension d-MI-180/12. The dependence of the critical frequency on the viscosity of the carrier fluid was analyzed applying a constant field on suspensions with different glycerol concentrations (d-MI-70/60a). We found that the critical frequency increases linearly with the square of the magnetization and decreases with the inverse of the viscosity, so the Mason number governs the dynamics. As expected from this result, we obtained a good collapse of the dichroism and the phase lag curves (measured at different magnetic fields and viscosities) with Mason number (see Fig. 1). The change in behavior of the dichroism and the phase lag occurs at a critical Mason number, $Ma_c \sim 1$, above which the viscous forces dominate and inhibit the aggregation process, being this one the mechanism responsible for the decrease of dichroism.

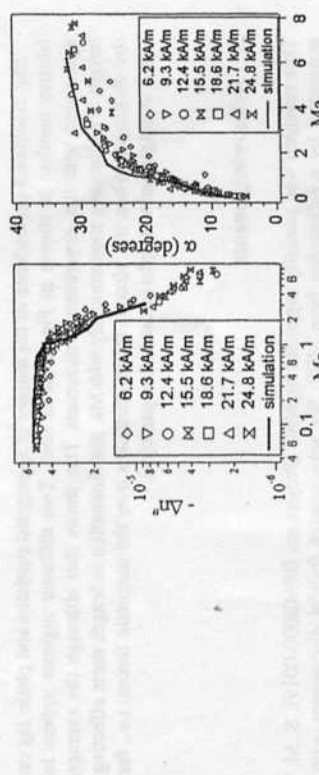


Figure 1. Collapse of dichroism (left) and phase lag (right) with Mason number for different magnetic field strengths. Suspension d-M1-180/12. Experimental results (markers), simulation results (solid line).

3.2 Video microscopy Results

In Fig. 2 video microscopy images show the behavior of the structures induced in the d-M1-070/6b suspension when we applied a magnetic field of $H = 1.55 \text{ kA/m}$ for two rotational frequencies corresponding to Mason numbers $\text{Ma} = 1.2 \cdot 10^{-3}$ (right) and $\text{Ma} = 1.2$ (left). These images were taken 300 sec after applying the magnetic field. Direct observations show that chains rotate synchronously with the field adjusting their size to decrease their viscous drag. The average size of the aggregates decreases with frequency following a power law behavior with an exponent close to -0.5, the same exponent predicted by the chain model developed by Martin et al. for ER fluids subject to steady shear [14]. For $\text{Ma} < 1$, although the length of the chains decreases with frequency, the number of aggregated particles (dichroism) remains almost constant supporting the scattering dichroism experimental findings.

Once the critical Mason number is surpassed, the viscous forces start to dominate the magnetic ones and the aggregation process is inhibited. Furthermore, for $\text{Ma} > 1$, the magnetic field is not strong enough for the structures to remain aligned in the field direction when rotating at these high frequencies and more isotropic structures are formed (see $\text{Ma} = 1.2$ in Fig. 2). These two mechanisms, the increase of the number of isolated particles and the formation of more isotropic structures, contribute to the decrease of the dichroism.

Fragmentation and aggregation processes are observed at low frequencies (Mason numbers below the critical value). As an example, the break up process of a chain rotating on a magnetic field with frequency $f = 0.01 \text{ Hz}$ is shown in Fig. 3. First the chain is bent (left picture), then it develops an S shape with the arms moving faster to follow the field (middle picture). Ultimately, the chain breaks up into smaller pieces (right picture). This S shape has been also reported for chains subject to shear in the direction perpendicular to the field [14], and also for magnetic droplets under rotating fields [4].

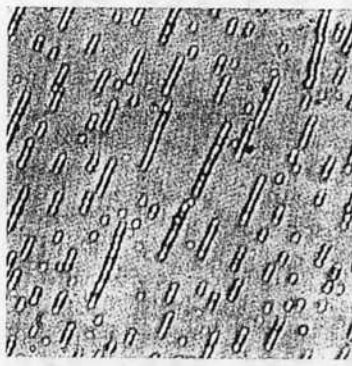


Figure 2. Video-microscopy images recorded after 300 s of applying a magnetic field with amplitude $H = 1.55 \text{ kA/m}$ for two rotational frequencies which correspond to $\text{Ma} = 0.0012$ (left) and $\text{Ma} = 1.2$ (right). We used suspension d-M1-070/6b. Field of view: $53 \times 53 \mu\text{m}$.



Figure 3. Detail of the S shape of a chain induced on the same suspensions when a magnetic field of amplitude $H = 1.55 \text{ kA/m}$ rotates counter clockwise with $f = 0.01 \text{ Hz}$. Field of View: $14.4 \times 14.2 \mu\text{m}$

4 Simulations

In order to interpret the experimental results we conducted athermal molecular dynamics simulations in 2D for a system of $N=400$ spherical particles of radius a . The particles are considered as "hard" spheres with induced dipolar interactions and Stokes friction against the solvent. In our experiments, the ratio between the magnetic and thermal energies, $\lambda = W_m / (k_B T)$, is much larger than one. Therefore Brownian motion should have a negligible effect on the evolution of the structures [15]. Similar models have been previously used to simulate MRF fluids [16,17] as well as electrohydrological fluids [18]. Under these assumptions, the equation of motion for the i th particle can be written as follow:

$$\gamma \frac{d\mathbf{r}_i}{dt} = \mathbf{F}_i^m + \mathbf{F}_i^{ev} \quad (2)$$

where $\gamma = 6\pi\eta a$ is the Stokes drag coefficient for a solid sphere, and \mathbf{F}_i^m is the magnetic force in dipolar approximation. Note that the inertial term was neglected because the viscous drag term dominates. As we are using one-particle Stokes' hydrodynamics, an excluded-volume repulsive force, \mathbf{F}_i^{ev} , must be included to keep particles from overlapping. This force is calculated as in ref. [16]. Making the above equation

dimensionless, a couple of scaling parameters immediately drop out. A spatial scale $r_1=2$ a , and a time scale $t_1=12^2 \eta / (\mu_0 M^2)$. This time scale leads to a dimensionless rotating frequency equal to the Mason number defined in Eq. (1). The same procedure has been reported in several works [17-19].

The simulations reveal that the magnetic dipolar interaction induces the formation of chainlike structures that follow the magnetic field rotating with the same frequency in agreement with the experimental findings. In Fig. 4 we plot the particles position in the XY plane for different frequencies (Mason numbers) at an arbitrary time. As demonstrated in this figure, the size of the structures becomes smaller as the rotating frequency increases. This indicates that hydrodynamic friction forces overcome the dipolar magnetic forces and therefore the chains break up to decrease their viscous drag.

According to the simulations, the average length of the chains decreases with frequency, scaling as the inverse square root of the Mason number (power law exponent equal to -0.45). This value is very close to the value obtained on the video microscopy experiments.

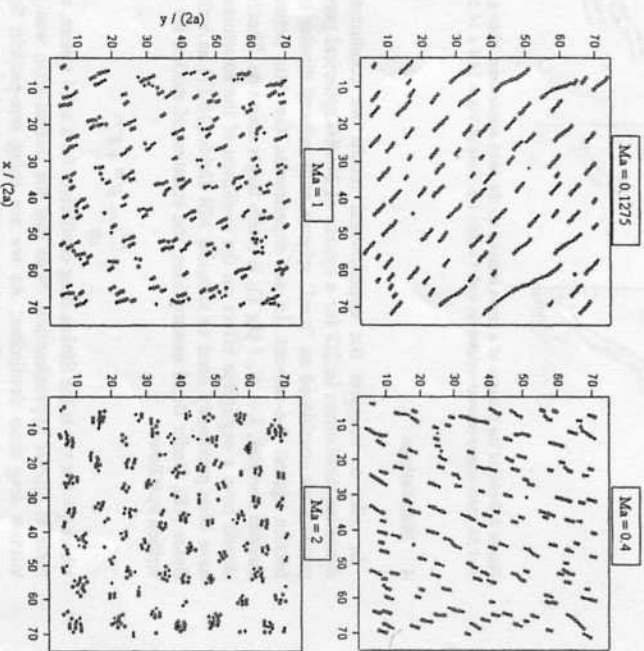


Figure 4. Dimensionless particles positions for different Mason numbers at an arbitrary time. Calculations for suspension d-MI-180/12.

The calculated dependence of the number of aggregated particles and phase lag on Mason number is shown in Fig. 1 (solid line). Two different regimes appear in agreement with the experimental dichroism. This shows that although the average length is decreasing monotonously with Ma, this diminution in length starts affecting the dichroism when the viscous forces dominates over the magnetic forces, i.e., for small average chain lengths (close to two particles).

5 Acknowledgements

This research was partially supported by MEC (Project no. BFM2000-0019). S. M. Was supported by a fellowship from MEC. We acknowledge fruitful discussions with J.E. Martin, P. Espanol, and I. Zuñiga.

References

1. Helgesen G., Pieranski P., and Skjeltorp A.T., *Phys. Rev. Lett.* **64** (1990) pp. 1425.
2. Helgesen G., Pieranski P., and Skjeltorp A.T., *Phys. Rev. A* **42** (1990) pp. 7271.
3. Bacri J.-C., Cébers A., and Perzynski R., *Phys. Rev. Lett.* **72** (1994) pp. 2705.
4. Sandre O., Browaeys J., Perzynski R., Bacri J.-C., Cabuil V., and Rosenzweig R.E., *Phys. Rev. E* **59** (1999) pp. 1736.
5. Martin J.E., Anderson R.A., and Tigges C.P., *J. Chem. Phys.* **108** (1998) pp. 7887.
6. Martin J.E., Anderson R.A., and Tigges C.P., *J. Chem. Phys.* **110** (1999) pp. 4854.
7. Martin J.E., E. Venturini, I. Odinek, and R.A. Anderson, *Phys. Rev. E* **61** (2000) pp. 2818.
8. Melle S., Fuller G.G., and Rubio M.A., *Phys. Rev. E* **61** (2000) pp. 4111.
9. Melle S., Calderón O.G., Fuller G.G., and Rubio M.A., *J. Coll. Inter. Sci.* (submitted).
10. Mason number was first introduced in literature for ER fluids under steady shear. See Gast A.P., and Zukoski C.F., *Adv. Colloid Interface Sci.* **30** (1989) 153.
11. Volkova O., Cutillas S., and Bossis G., *Phys. Rev. Lett.* **82** (1999) 233.
12. Martin J.E., *Phys. Rev. E* **63** (2000) pp. 011406.
13. Fuller G.G., *Optical rheometry of complex fluids*, Oxford University Press (1995).
14. Martin J.E., and Anderson R.A., *J. Chem. Phys.* **104** (1996) pp. 4814.
15. Martin J.E., Venturini E., Odinek J., and Anderson R.A., *Phys. Rev. E* **61** (2000) pp. 2818.
16. Mohebi M., Jannabi N., and Liu J., *Phys. Rev. E* **54** (1996) pp. 5407.
17. Martin J.E., Anderson R.A., and Tigges C.P., *J. Chem. Phys.* **108** (1998) pp. 3765 and pp. 7887.
18. Klingenber D.J., Swol F. van, and Zukowski C.F., *J. Chem. Phys.* **91** (1989) pp. 7888.
19. Larson R.G., *The structure and Rheology of Complex Fluids*, Oxford University Press, New York, 1999.